Reversing the stereochemistry of a Diels–Alder reaction: use of metalloporphyrin oligomers to control transition state stability

Zöe Clyde-Watson, Anton Vidal-Ferran, Lance J. Twyman, Christopher J. Walter, Duncan W. J. McCallien, Stefano Fanni, Nick Bampos, R. Stephen Wylie and Jeremy K. M. Sanders*

Cambridge Centre for Molecular Recognition, University Chemical Laboratory, Lensfield Road, Cambridge, UK CB2 1EW

A cyclic Zn-porphyrin trimer with ethyne and butadiyne links stabilises the thermodynamically disfavoured *endo* transition state and product of a reversible Diels–Alder reaction; at 30 °C the *endo* adduct is formed rapidly and almost exclusively. Linear porphyrin dimers containing ethyne or butadiyne links show related stereochemical preferences to the corresponding cyclic trimers; substantial rate accelerations are observed despite rotational freedom around the linkers. A qualitative correlation is observed between rate acceleration (*i.e.*, transition state binding) and product binding, and the results are rationalised in terms of host geometry and flexibility.

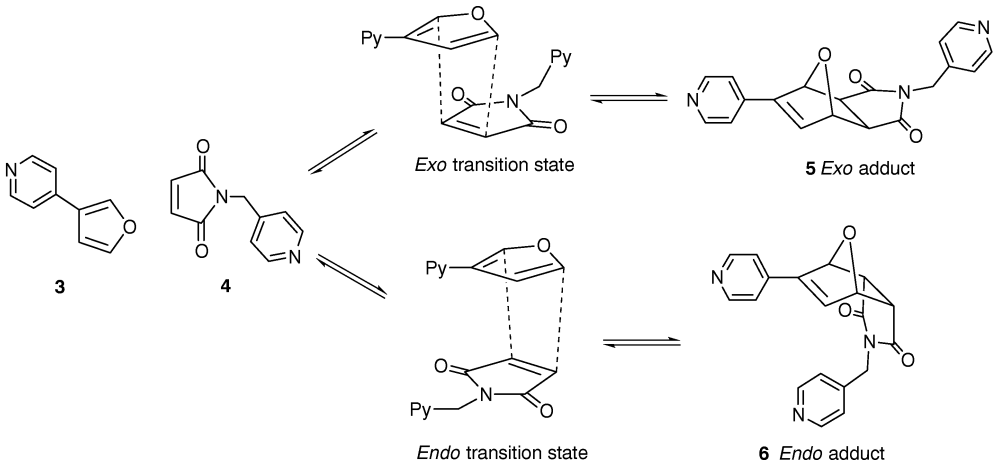

Scheme 1 Reversible Diels–Alder reaction between diene **3** and dienophile **4** to give *exo* adduct **5** and *endo* adduct **6**

One of the key aims of supramolecular chemistry is to catalyse unfavourable reaction pathways. There are several reports of the use of catalytic antibodies[1] and cyclodextrins[2] to catalyse unfavourable stepwise reactions, but at present there are no examples of the use of designed, specific host-guest binding to control pericyclic reaction geometry. We now report a small but significant step in that direction by demonstrating that the 1,1,2-linked[3] cyclic porphyrin trimer $\mathbf{Zn_3 1}$ can reverse the stereochemical outcome of a Diels–Alder reaction within its cavity by selectively accelerating the thermodynamically and kinetically disfavoured *endo* reaction pathway. Furthermore, we show that linear porphyrin dimers possessing rotational freedom between their two binding sites retain similar stereochemical selectivity and surprisingly large rate accelerations. Previous examples of redirected pericyclic reactions either involved non-directional binding[4,5] or catalytic antibodies developed using appropriate transition state analogues.[6]

* Email:jkms@cam.ac.uk

The Diels–Alder reaction possesses a number of features that make it an attractive target for supramolecular manipulation: it is a bimolecular process; it requires no external reagents; it proceeds through a highly ordered transition state that resembles the product (Scheme 1);[7] and it offers the opportunity for changing the stereochemical and regiochemical outcome by selective stabilisation of a disfavoured transition state. All Diels–Alder reactions are reversible, but often the reverse process is so slow that it is not observed. The *endo* adduct is usually the kinetic product, the transition state being stabilised by secondary π-orbital interactions; reactions that are effectively irreversible therefore tend to give predominantly the *endo* adduct. However, the *exo* adduct is generally sterically and electronically favoured, and tends to be the dominant product in reversible thermodynamically controlled reactions. Not surprisingly, the Diels–Alder reaction has been the subject of many supramolecular studies exploiting systems as diverse as micelles,[8] synthetic hosts in solution,[5,9,10] crystalline hosts in the solid state[11] and catalytic antibodies.[6,12]

Our approach to biomimetic catalysis has been to create synthetic systems in which convergent binding sites are positioned in such a way that substrate molecules can be held in close proximity.[13,14] In principle such hosts should catalyse reactions simply by virtue of their binding properties: the unfavourable entropy of activation would be reduced or compensated for by the favourable enthalpy of binding. Porphyrin hosts such as **$Zn_3$1** and **$Zn_3$2** can bind pyridine-based ligands within the cavity; if these ligands are relatively rigid then the high effective concentration generated by their binding should be conveyed efficiently to the reactive site. Our long-term design strategy has been to create a series of receptors using the same diarylporphyrin building block but exploring different metal recognition properties and a range of cavity shapes and sizes. In this way we may dissect out the different contributions to binding and catalysis and influence the outcome of reactions with multiple pathways.

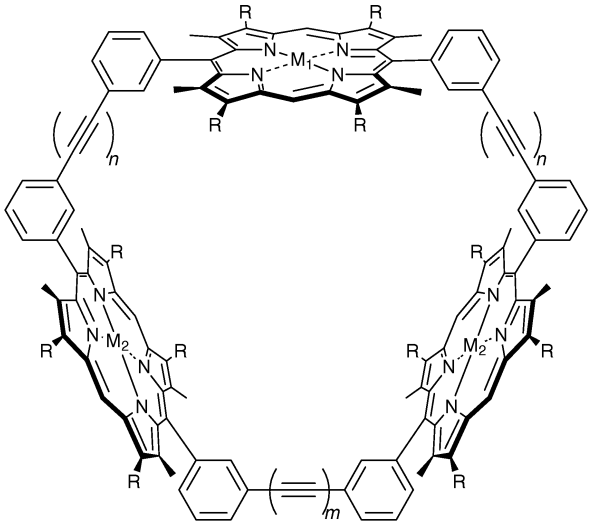

$Zn_3$1 $n = 1, m = 2; M_1 = M_2 = Zn;$ R = CH_2CH_2COOMe

Zn_2Ni1 $n = 1, m = 2; M_1 =$ Ni, $M_2 = Zn;$ R = CH_2CH_2COOMe

$Zn_3$2 $n = m = 2; M_1 = M_2 = Zn;$ R = CH_2CH_2COOMe or Et

Initially, we chose to study the reaction of the furan-derived diene **3** with the maleimide-derived dienophile **4** (Scheme 1) within the large cavity of our first generation host, the 2,2,2-trimer **$Zn_3$2**. Model building suggested that the substrates bind in an orientation that closely approaches the *exo* transition state, and precedent[7] showed that this Diels–Alder process is reversible. This reversibility offered the opportunity to study the kinetics, and therefore the approach to the transition state, in both the forward and reverse directions. In the event, the symmetrical 2,2,2-linked **$Zn_3$2** is so selective in accelerating the formation of the thermodynamically more stable *exo* adduct **5** that no *endo* adduct **6** can be detected at any stage in the time course.[15–18] Under the reaction conditions macroscopic accelerations of several hundred-fold are observed,[19] but no catalytic turnover is obtained or expected because the product will bind strongly and inhibit further substrate binding. In the first instance our objective was to control the stereochemical outcome of the reaction, and in such circumstances the rôle of the host is more like that of a chiral auxiliary than that of a catalyst. Above room temperature, this particular *endo* adduct is disfavoured both kinetically and thermodynamically.[17,18]

The selectivity observed in the 2,2,2-linked trimer originates in its geometrical complementarity to the *exo* adduct and transition state; modelling indicates an N—N distance of

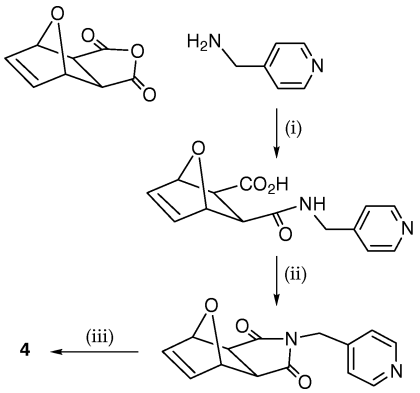

Scheme 2 Synthesis of dienophile **4**. (i) THF, 25 °C, 12 h; (ii) HOBT, DCC, CH_2Cl_2 ; (iii) 160 °C, 15 mm Hg

around 13 Å and a Zn—Zn distance of *ca.* 15 Å, allowing formation of two good Zn—N bonds in the 1 : 1 complex. In other words, stabilisation of the *exo* transition state and adduct leads to selective acceleration of the reaction. However, the predicted N—N distance in the optimum binding geometry of *endo* adduct **6** is only 9 Å, so the fit is poor. At 60 °C in tetrachloroethane solution, the binding energy for the *endo* adduct is *ca.* 1 kJ mol^{-1} less favourable than for the diene and dienophile binding independently and 5 kJ mol^{-1} less favourable than for the *exo* adduct.[18] By contrast, the 1,1,2-trimer[20,21] **$Zn_3$1** encloses a smaller and more rigid cavity characterised by two distinct Zn-porphyrin environments and distances. The Zn—Zn distance across the butadiyne linkage is expected to be 15 Å, as in the 2,2,2-trimer, while across the ethyne bridge it should be only 12 Å and therefore more complementary to the *endo* adduct.

The results reported here confirm that indeed the smaller binding site formed by two ethyne-linked porphyrins is capable of stabilising both the *endo* transition state and product, thereby reversing the 'natural' stereochemistry of the reaction. However, the results also indicate that less tangible factors of host and substrate flexibility also play vital rôles that are much more difficult to predict.

Results

Syntheses

Diene **3** was originally prepared here by a rather indirect method,[22] but we have since found it to be much more reliable to couple 3-bromofuran with 4-trimethylstannylpyridine using $[PPh_3]_4Pd$. As **3** is an oil, it was converted to its crystalline hydrochloride salt for convenient storage and handling of small quantities. Dienophile **4** was prepared by the route shown in Scheme 2. The adducts **5** and **6** were prepared for binding studies by the Diels–Alder reaction of **3** and **4**, as described previously.[17] However, multimilligram quantities of pure *endo* adduct **6** were difficult to obtain: at low temperatures the reaction is extremely slow (>10 days) and produces mostly *exo* adduct **5**, which is nontrivial to separate from **6** chromatographically. Above room temperature the *endo* adduct **6** is unstable in solution, reverting to component diene and dieneophile, which can then recombine to give **5**; attempts to concentrate solutions of the *endo* adduct, *e.g.*, by rotary evaporation at room temperature, therefore tend to lead to significant contamination by **5**. Isolation of preparative quantities of pure **6** from a selective host-accelerated reaction was subject to the same difficulties.

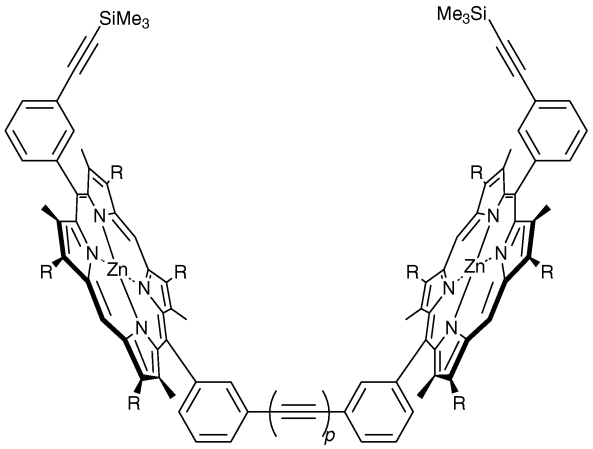

$Zn_2$7 p = 2; R = CH_2CH_2COOMe

$Zn_2$8 p = 1; R = CH_2CH_2COOMe

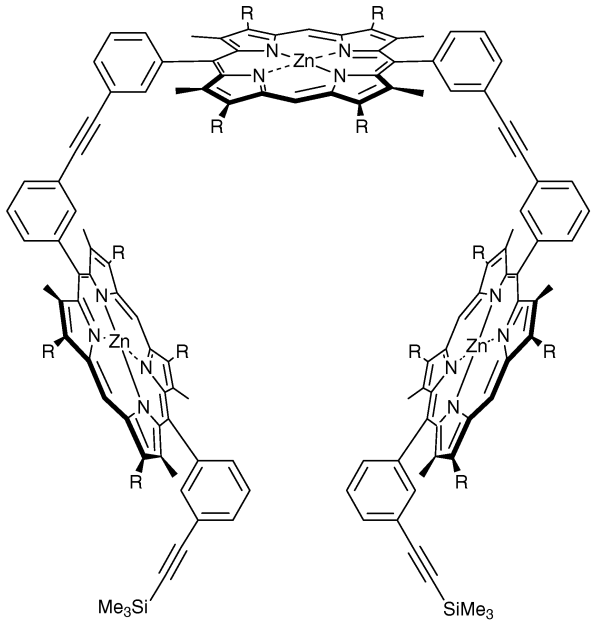

$Zn_3$12 R = CH_2CH_2COOMe

The large 2,2,2-trimer **$Zn_3$2** and butadiyne-linked dimer **$Zn_2$7** were prepared using published methods,[23] while the shorter ethyne-linked dimer **$Zn_2$8** was prepared in 68% yield by Pd^0-catalysed coupling of monomers **Zn9** and **Zn10**; synthesis of these monomers has been described previously.[21,23] Hydrogenation of **$Zn_2$8** gave the flexible linear dimer **$Zn_2$11**.[24] The smaller cyclic 1,1,2-trimer **$Zn_3$1** was prepared by templated Glaser–Hay cyclisation of linear trimer **$Zn_3$12**, which was itself synthesised by two different routes: originally[21] the Pd^0-catalysed coupling of monomer **Zn13** with two equivalents of **Zn9** was employed, but chromatographic purification of **Zn9** on a large scale is far from trivial, and recent experience has shown that it is more convenient to couple the diiodo monomer **Zn14** with two equivalents of **Zn10**.

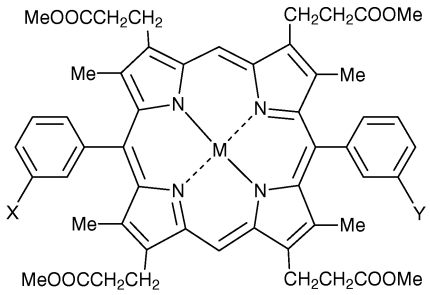

Zn9 X = C≡C–$SiMe_3$; Y = I

Zn10 X = C≡C–$SiMe_3$; Y = C≡C–H

Zn13 X = Y = C≡C–H

Zn14 X = Y = I

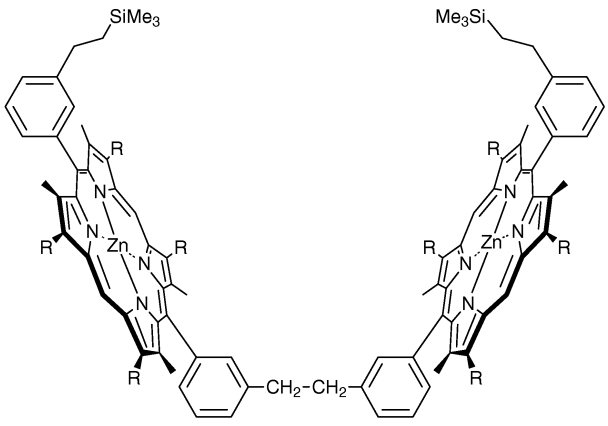

$Zn_2$11 R = CH_2CH_2COOMe

Kinetic studies

Solubility considerations and the slow rate of the reaction at room temperature dictated that the Diels–Alder reaction was carried out in tetrachlorethane at a concentration of 0.9 mM for each of the substrates and the porphyrin host. FTIR spectroscopy was effective at measuring overall accelerations but was unable to distinguish *exo* from *endo* adducts. Gas chromatography was found to be unsuitable due to thermal reversal of the products to starting materials in the injector port. HPLC and UV spectroscopy suffered from the disadvantage that the host must be removed from the reaction mixture before assay.

In the event, therefore, ^{1}H NMR spectroscopy was adopted as the assay technique, although this also proved not to be ideal: at the concentration at which the reaction is carried out, the proportion of both monodentate reactants and bidentate products bound to the host at any one time is substantial; these proportions also change during the course of the reaction. The combination of exchange broadening and time-dependent shifts in the presence of binding sites rendered it necessary to demetallate each aliquot removed from the reaction mixture before the ratio of the various signals could be obtained by NMR spectroscopy. In order to achieve this, a standard amount of TFA–MeOD was added to each aliquot, followed by one drop of 100% deuteriopyridine to ensure complete neutralisation. The relative amounts of the two adducts could be quantified ($\pm$ 5%) by integration of a characteristic *exo* signal at 6.92 ppm and *endo* signals at 6.84 and 6.94 ppm. This procedure, carried out in duplicate on parallel samples, gave reproducible *exo* : *endo* proportions and semi-quantitative values for reaction rates. However, the rate data presented below should be taken as indicative rather than definitive.

Control reactions in the absence of hosts were so slow that the rate constants summarised in Table 1 were measured with 9 mM substrates; NMR spectroscopy was used for these rate

Table 1 Rate constants of *exo* and *endo* reactions in tetrachloroethane in the absence of host

	30 °C		60 °C	
	Exo	*Endo*	*Exo*	*Endo*
Forward/ $mol^{-1}\ dm^3\ s^{-1}$	$3.1(\pm0.6) \times 10^{-5}$	$1.5(\pm0.3) \times 10^{-5}$	$2.2(\pm0.4) \times 10^{-4}$	$5(\pm2) \times 10^{-5}$
Reverse/s^{-1}	$<6 \times 10^{-9}$	$<6 \times 10^{-9}$	$5.5(\pm1.1) \times 10^{-7}$	$3.1(\pm0.6) \times 10^{-5}$

measurements as there were no complications from host-induced effects. In the absence of host at 30 °C, the *exo* : *endo* proportion is *ca.* 2 : 1; at 60 °C the initial *exo* : *endo* ratio is *ca.* 4 : 1, but the much faster reverse reaction of the *endo* adduct soon leads to complete loss of this product in favour of the *exo* adduct, making measurement of the forward rate very imprecise.

The reaction in the presence of the various hosts was studied at 30 and 60 °C. Preliminary studies had indicated that the macroscopic rate of the reaction in the presence of 2,2,2-trimer was relatively temperature independent: raising the temperature leads to lower binding constants but faster intrinsic reactions, and for the trimer these effects roughly cancel out in the accessible temperature range.[16] As the temperature dependence of the reverse reaction rates and binding constants to hosts were rather different for the two adducts, we hoped to see temperature-dependent outcomes for host accelerations. This hope was indeed realised in practice, and Table 2 summarises the qualitative aspects of the observed *exo* : *endo* selectivity. Table 3 summarises the observed rate accelerations for each adduct relative to the rate of formation of that adduct in the absence of host.

At 30 °C, in contrast to any of the other cyclic hosts we have studied, the 1,1,2-trimer **$Zn_3$1** is totally *endo*-selective: no trace of any *exo* adduct was detected by ^{1}H NMR spectroscopy at any stage of the reaction. As Fig. 1 shows, the macroscopic reaction rate achieved by **$Zn_3$1** is somewhat smaller than that achieved by the 2,2,2-trimer **$Zn_3$2**, but the stereochemical outcome of the reaction is completely reversed, despite the *endo* reaction being intrinsically slower than the *exo*.

In the presence of 1,1,2-trimer at 60 °C, the *endo* and *exo* adducts are formed in essentially the same proportions at the beginning of the reaction: after 10 h the yield of each adduct is around 20% (Fig. 2). However, the yield of *endo* adduct then reaches a peak of around 24% and then as the reaction proceeds towards equilibrium, the amount of *endo* adduct drops below that of the *exo* adduct, eventually reaching *ca.* 10%. Nevertheless, thermodynamic stabilisation provided by the 1,1,2-trimer cavity gives a long lifetime to a product that otherwise simply decomposes by reverse reaction at this temperature.

The obvious interpretation of this result is that the *endo* geometry is stabilised by binding to two porphyrins across the ethyne linkage. In an attempt to confirm this, the effect of **Zn_2Ni1** was briefly examined at 60 °C. Nickel porphyrins generally bind much more weakly than their Zn analogues to pyridines, so we predicted that **Zn_2Ni1** would be ineffective at accelerating the *endo* reaction. This proved to be only partly correct: as expected the *exo* adduct now dominates, but is formed at only half the rate observed with **$Zn_3$1** while some *endo* adduct is formed, reaching a maximum of 10% after 45 h before dying away and being replaced by *exo* adduct. We have observed unexpectedly strong, spatially-enforced binding of the tridentate ligand tripyridyltriazine to the Ni centre in **Zn_2Ni1**[21] and presume that a similar effect is operating here, enhancing the binding of bidentate adducts across the ethyne linkage to the Ni centre. This result obscures what would otherwise be a straightforward control experiment. A better control would be to use the host resulting from cyclisation of the Zn—freebase—Zn linear trimer **12**, but this synthesis has never succeeded even in the most experienced hands.[25] The reasons for this and consistent failures of the cyclisation step in related systems are unclear, but they appear to be connected with deformations (or the deformability) of the central

Table 2 Summary of host-induced stereoselectivities[a]

Host	Product selectivity at 30 °C	Product selectivity at 60 °C
None	*exo* + *endo*	*exo* + transient trace *endo*
1,1,2-Trimer **$Zn_3$1**	*endo*	*exo* + *endo*
2,2,2-Trimer **$Zn_3$2**	*exo*	*exo*
Ethyne-linked dimer **$Zn_2$8**	*exo* + *endo*	*exo* + *endo* (trace)
Butadiyne-linked dimer **$Zn_2$7**	*exo*	*exo*
$-CH_2CH_2-$ linked dimer **$Zn_2$11**	—	*exo*

[a] Initial concentrations of diene, dienophile and host were 0.9 mM in tetrachloroethane.

Table 3 Host-induced macroscopic initial rate accelerations[a]

	Rate acceleration at 30 °C		Rate acceleration at 60 °C	
Host	*Exo*	*Endo*	*Exo*	*Endo*
1,1,2-Trimer **$Zn_3$1**	—	500	50	200
2,2,2-Trimer **$Zn_3$2** (ester)	1500	—	680	—
2,2,2-Trimer **$Zn_3$2** (ethyl)	1000	—	200	—
Ethyne-linked dimer **$Zn_2$8**	15	25	15	—
Butadiyne-linked dimer **$Zn_2$7**	80	—	30	—
$-CH_2CH_2-$ linked dimer **$Zn_2$11**			3	—

[a] Relative to rates in the absence of host. Initial concentrations of diene, dienophile and host were 0.9 mM in tetrachloroethane.

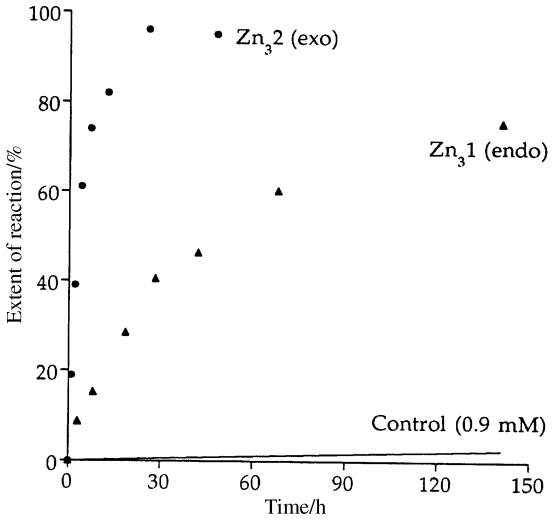

Fig. 1 Progress of the Diels–Alder reaction in Scheme 1 at 30 °C in tetrachloroethane solution in the presence of **$Zn_3$1** (only *endo* adduct observed) or **$Zn_3$2** (only *exo* adduct observed). Host, diene and dienophile were initially present at 0.9 mM concentration. Also shown is a progress curve for the control reaction (*exo* plus *endo*) calculated from measurements at higher concentration[15,16]

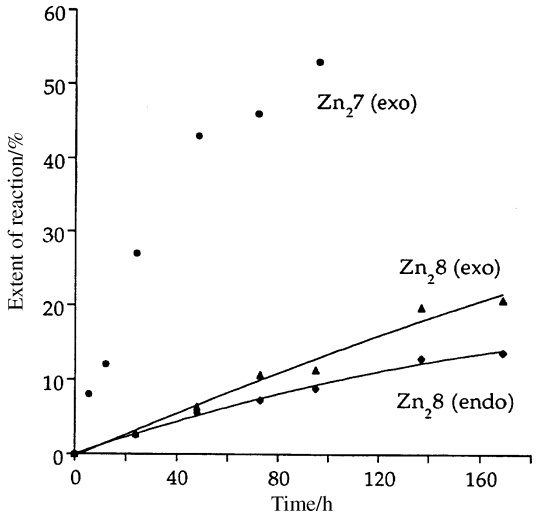

Fig. 3 Progress of the Diels–Alder reaction at 30 °C in tetrachloroethane solution in the presence of the linear dimers **$Zn_2$7** (only *exo* observed) and **$Zn_2$8** (*exo* and *endo* adducts shown separately)

porphyrin and with the lack of flexibility of the resulting macrocycle, as discussed below.

In order to confirm more directly the idea that the *endo* geometry is stabilised by binding to two porphyrins across the ethyne linkage while the *exo* geometry is stabilised by binding across the butadiyne linkage, we turned to the linear dimers **$Zn_2$7** and **$Zn_2$8**. At 30 °C the product distribution is roughly 3 : 2 *exo* : *endo* in the presence of ethyne-linked **$Zn_2$8** (Fig. 3) and significant rate enhancement is achieved; the butadiyne-linked **$Zn_2$7** shows complete *exo* selectivity at 30 °C and very substantial rate enhancement. At 60 °C the ethyne-linked **$Zn_2$8** does not alter the product distribution significantly relative to the 60 °C control and the overall acceleration decreases dramatically: only a very small proportion of the *endo* adduct is detected and this drops after 48 h, whereafter only the *exo* adduct can be observed. This resembles the behaviour of the 1,1,2-trimer at 60 °C and again is attributed to the large intrinsic rate of the *endo* back-reaction at 60 °C. The butadiyne-linked dimer **$Zn_2$7** at 60° C gives only the *exo* adduct, which is unsurprising in the light of the 30 °C behaviour.

Given the rotational freedom of these linear dimers, the large rate enhancement observed is remarkable; presumably the success of these hosts can be partially attributed to the rigidity of the linker groups restricting the conformational space available to the porphyrin units. This is confirmed by the observation that in the presence of the more flexible dimer **$Zn_2$11** at 60 °C the reaction was much slower than with the previous linear dimers. It was a much longer period of time before any *exo* adduct could be detected. No *endo* adduct was observed at all during the experiment, which is not surprising given the dominance in previous experiments of the thermodynamic *exo* product after an extended period at this temperature. At 30 °C the reaction with the flexible dimer was too slow to monitor in a practical way.

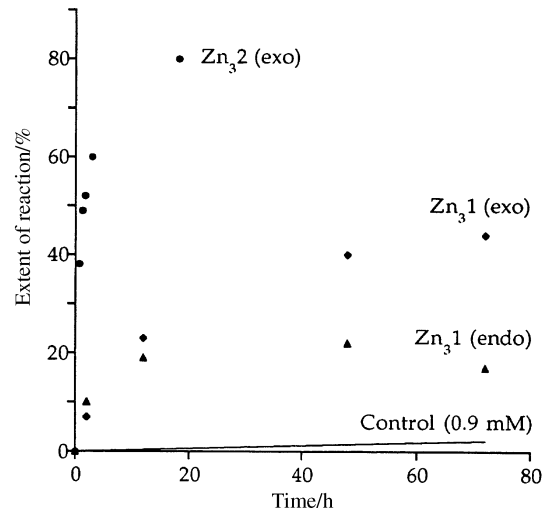

Fig. 2 Progress of the Diels–Alder reaction at 60 °C in tetrachloroethane solution in the presence of **$Zn_3$1** (*exo* and *endo* adducts shown separately) or **$Zn_3$2** (only *exo* observed). Also shown is a progress curve for the control reaction (*exo* plus *endo*) calculated from measurements at higher concentration[15,16]

Binding studies

The strengths of the various host–product interactions were gauged by UV/VIS titrations in the usual way:[26] on binding pyridine, the main Soret absorption band of zinc porphyrins experiences a 10 nm bathochromic shift, which can be monitored in a spectrophotometric titration to yield association constants. Two weak solutions of host are made up ($\approx 10^{-6}$ M), one of which contains the appropriate ligand at a much higher concentration (≈ 0.05 M). The latter solution is added in known portions to the pure host solution and the absorption intensities are monitored at the wavelengths of maximum intensity change, *i.e.*, at λ_{max} for the Soret bands of the unbound host and of the bound complex. The binding constants can be derived using a Simplex least-squares curve-fitting program and a plausible model for the stoichiometry of the host–guest interaction. At 30 °C in tetrachloroethane, the diene binds to the various hosts with a binding constant of around 2000 M^{-1}, falling to around 500 M^{-1} at 60 °C; binding constants for the dienophile are around half as strong due to the electron-withdrawing maleimide substitution.[27]

The analysis can become more complicated for the binding of multidentate ligands to hosts with multiple binding sites. In the case of an *n*-dentate ligand binding to a host with *n* binding sites, only the macroscopic binding constant may be measured and not that of any of the individual ligand interactions. A further complication arises when an $(n - x)$-dentate ligand binds to an *n*-dentate host, for example in the binding of a bidentate ligand to a tridentate receptor. A bidentate ligand will first bind to two sites, providing the geometry is appropriate, after which a second ligand molecule will bind

Table 4 Selected binding constants measured in tetrachloroethane

	K/M^{-1} at 30 °C		K/M^{-1} at 60 °C	
Host	*Exo*	*Endo*	*Exo*	*Endo*
1,1,2-Trimer $\mathbf{Zn_3}$**1**	3×10^5	4×10^6	2×10^5	1×10^5
2,2,2-Trimer $\mathbf{Zn_3}$**2** (ester)	2×10^7	2×10^6	nd[a]	nd[a]
2,2,2-Trimer $\mathbf{Zn_3}$**2** (ethyl)	9×10^6	6×10^5	4×10^5	8×10^4
Ethyne-linked dimer $\mathbf{Zn_2}$**8**	3×10^5	5×10^5	9×10^4	3×10^4
Butadiyne-linked dimer $\mathbf{Zn_2}$**7**	1×10^6	1×10^5	6×10^5	1×10^5
$-CH_2CH_2-$ linked dimer $\mathbf{Zn_2}$**11**	1×10^5	1×10^5	1×10^4	1×10^4

[a] Not determined.

monodentately to the third binding site. In all the cases described here, sufficiently low concentrations of ligands were used such that there was no interference from complexes of stoichiometry other than 1 : 1, but the experiment cannot distinguish binding at non-equivalent sites within one host.

Table 4 summarises the product binding constants measured as described above. Note, however, that the problems associated with obtaining the *endo* adduct and working with it at 60 °C limit the reliability of its binding constants to order-of-magnitude estimates.

Discussion

The *exo* selectivity and large rate acceleration induced by the cyclic 2,2,2-trimer[15–18] raised two obvious questions. (*i*) Can the stereochemical selectivity be reversed by use of a suitable host? (*ii*) Would an acyclic system of the same potential geometry show any activity? The results presented here provide emphatically positive answers. The ability, at 30 °C, of the 1,1,2-trimer to completely reverse the stereochemical outcome of the Diels–Alder reaction, and of the rotationally-free linear dimer $\mathbf{Zn_2}$**7** to induce *exo*-selective accelerations as large as 80-fold, are satisfying examples of the power of designed host–guest interactions to influence chemical outcomes.

However, design does not always lead to the expected result, especially where access to the desired host is frustrated by synthetic problems: the small 1,1,1-trimer was a prime synthetic target for some time, as it was expected to be *endo*-selective by virtue of geometry and amenable to quantitative kinetic studies by virtue of its symmetry. In the event, substantial quantities of this material proved elusive despite the exploration of several different synthetic routes.[28,29] No serious binding or kinetic studies were possible, but a single experiment at 60 °C showed that it accelerates the Diels–Alder reaction effectively and with considerable (but not exclusive) *endo* selectivity, as expected.

The 1,1,2-trimer system was, therefore, initially conceived as an alternative "small" cavity. The convergent synthetic route, especially incorporating the improvement described in this paper, has proved to be extremely versatile. It has allowed access to trimers containing well-defined combinations of metals such as Zn, Ni, Ru and Sn, and to combinations of building blocks such as dioxo- and nitroporphyrins,[30] although as pointed out above the cyclisation step fails consistently for the Zn—freebase—Zn trimer and some other systems, for reasons that are unclear.

The asymmetry generated by the unique environment of the "northern" porphyrin is a rich source of geometrical information for ligands that bind extremely strongly within the cavity,[20,21,29] but it makes any quantitative analysis of binding and kinetics in the present Diels–Alder investigation almost impossible: for example, the overall binding constants cannot be separated into K_{ethyne} and $K_{butadiyne}$ components. There are too many binding constants and rate constants (forward and reverse, across ethyne and across butadiyne, *endo* and *exo*) in this system to allow meaningful simulation of the entire reaction scheme and construction of a free-energy profile. With so many variables it has not been possible to find a unique and reliable fit to the experimental data using a simulation program,[31] so our discussion is mainly restricted to the qualitative aspects.

The Diels–Alder results at 30 °C for the two cyclic trimers can be summarised in the cartoon shown in Fig. 4: the *endo* adduct shows a high complementarity to the porphyrin binding sites across the shorter ethyne-linker while the *exo* adduct is more complementary to the longer butadiyne-linked binding site. At 30 °C the 1,1,2-trimer produces only *endo* adduct so it must lower the free energy of the *endo* transition state to below that of the *exo* even though intrinsically the *endo* transition state is slightly higher in energy. Assuming that total amount of *exo* adduct produced is less than ≈ 3% (the minimum amount detectable by the ^1H NMR assay), the

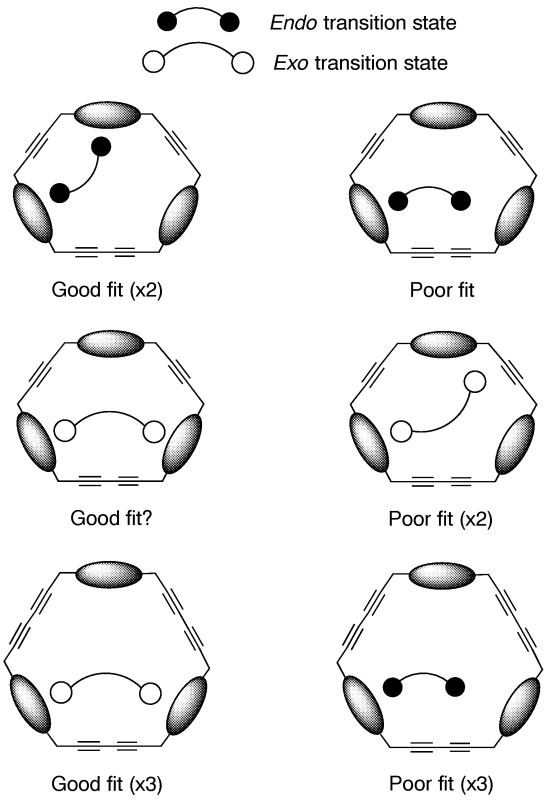

Fig. 4 Cartoon representation of the fit of the *endo* and *exo* transition states across the ethyne and butadiyne linkages of the cyclic hosts

endo reaction is faster than the *exo* reaction in this case by a factor of at least thirty. The *endo* acceleration is 500-fold, so the acceleration of the *exo* reaction pathway due to the 1,1,2-trimer is less than around 10-fold (remembering that the *exo* reaction is intrinsically twice as fast). This is a dramatic and unexpected difference from the 1500-fold acceleration seen with 2,2,2-trimer, even allowing for the presence of only one butadiyne-linked site rather than three.

The complete suppression of *exo* adduct in the 1,1,2-cavity in kinetic experiments at 30 °C is supported by the measured binding constants: a high affinity for the *endo* adduct is accompanied by remarkably weak binding of the *exo* adduct. The binding of *exo* adduct to the 1,1,2-trimer is around 60-fold weaker than to the 2,2,2-trimer, rather than the factor of three that one might expect. Model building and molecular modelling (Cerius[2]) give no reason to expect any significant equilibrium geometry difference across the butadiyne linkage in the two trimers, so one must conclude that the kinetics and binding are more sensitive probes for geometry in such large systems. We take up this question again below.

The picture at 60 °C for the 1,1,2-trimer is less clear in detail, but again *endo* acceleration by the ethyne-linked sites appears to be more effective than *exo* acceleration by the butadiyne-linked sites. An equimolar mixture of the *endo* and *exo* products is produced, corresponding to an acceleration of roughly 200-fold for the *endo* reaction, compared with the control *endo* reaction, and an acceleration of roughly 50-fold for the *exo* reaction compared with the *exo* control. Beyond twenty-four hours or so, the level of *endo* adduct drops significantly and the thermodynamic *exo* adduct begins to dominate. It is apparent that at 60 °C the *exo* transition state can take up a conformation that can bind bidentately within the cavity, so formation of this product is accelerated. It is not clear from this observation alone whether this binding is across the ethyne or butadiyne linkage, or a mixture, but 60 °C evidence from linear dimer **$Zn_2$8** and the 1,1,1-trimer suggests at least some *exo*-binding across the ethyne linkage. The greater thermodynamic stability of the *exo* adduct (*i.e.*, its much slower reverse reaction) means that this becomes the dominant product as the reaction approaches equilibrium.

To summarise the 1,1,2-trimer results, the geometry and size of the cavity favour the formation of the kinetic *endo* product at both temperatures, but at 60 °C this effect is largely masked by the increasing dominance of the thermodynamic *exo* product. Nevertheless, the persistence of the *endo* adduct at 60 °C can be attributed to stabilisation within the cavity by binding across the ethyne bridge.

The reversal of stereoselectivity between the two cyclic trimers at 30 °C is the result of two separate effects, one predicted and one not predicted: the large *endo* acceleration induced by the small trimer was expected and may be considered a success for the design approach. However, the fact that this trimer is so much less effective at 30 °C than the larger analogue at accelerating the *exo* reaction and binding *exo* adduct is a surprise. Perhaps the key difference lies in the greater flexibility of the larger 2,2,2-system: if a small change in host geometry is required for optimum binding of the *exo* adduct, it will be energetically less costly for the more flexible system. In other words, success requires mutuality: the 2,2,2-trimer is sufficiently flexible that it can respond better than the 1,1,2-trimer to the geometrical needs of the *exo* adduct. Certainly the flexibility of 2,2,2 is apparent both in its ligand binding properties[26] and in the fact that it is easier to prepare analogues with distorted dodecasubstituted porphyrins in the 2,2,2-series[32] than in the 1,1,2-series.[29] The binding constant between *exo* adduct and 2,2,2-trimer at 30 °C is large (Table 4) but is at least ten times smaller than for a ligand that is of optimum geometry.[26] This is additional evidence of a mismatch of ground state geometries.

We turn now to the linear dimers. The kinetic and thermodynamic stereoselectivity of the butadiyne-linked dimer **$Zn_2$7** are broadly as one would have expected from the 2,2,2-trimer: **$Zn_2$7** is geometrically complementary to the *exo* adduct and accelerates *exo* formation. For the ethyne-linked dimer **$Zn_2$8** the binding preference for the adducts is reversed, as expected: at 30 °C the *endo* adduct is bound marginally more strongly, but the *exo* reaction is intrinsically faster so both adducts are observed, while at 60 °C *exo* is preferred kinetically and thermodynamically. This behaviour at the higher temperature reflects that of the 1,1,2-trimer, and confirms that it is indeed possible at higher temperatures for the *exo* transition state to take up a conformation that can bind bidentately across the ethyne linkage; the large product binding constant supports this observation.

The rigidly linked linear dimers can rotate freely about the linker group axis but the trajectories followed by the porphyrin binding sites are constrained to be essentially circular. In order to accelerate the Diels–Alder reaction, the two porphyrin units must take up a limited range of conformations to allow the bound substrates to react. Consequently, the reaction is roughly 20-fold slower at 30 °C than for the trimers; on purely statistical grounds one would expect a three-fold reduction in the acceleration,[33] so the effective rate accelerations are only reduced by around seven-fold by rotational freedom. These large accelerations are consistent with the surprisingly large binding constants seen at 30 °C, corresponding to effective molarities of around 1 M for the favoured adducts: the entropic cost of restricting rotation around the linker must be effectively compensated by the enthalpic benefit derived from achieving ideal Zn—N bonding at both ends of the adducts.

Hydrogenation of the rigid linker to give **$Zn_2$11** greatly increases the amount of conformational space that the porphyrin units can explore, and may allow intramolecular self-association,[27] so it is not surprising that both binding and acceleration are so small. The ability of this host to bind either adduct with equal strength is a reflection of the conformational flexibility that enables it to wrap with equal facility around bidentate ligands of different geometries in order to maximise favourable binding interactions. The net energetic benefit of such binding is, however, weak because there is a very large entropic price to pay for restricting a highly flexible system. The potential of a particular host system to accelerate such a reaction is thus dependent on a delicate balance between two opposing factors: flexibility results in good binding but poor rate acceleration whereas rigidity may result in good rate acceleration (and in some cases stereoselectivity) but only if the geometry is precisely right.

Conclusion

Qualitatively, it has been possible to obtain a clear picture of the effects of cavity size and host geometry on this particular Diels–Alder reaction. We have shown that subtle changes in host design can lead to dramatic changes in the stereochemical outcome of a Diels–Alder reaction where there are two finely balanced pathways, and have demonstrated a qualitative correlation between rate acceleration (*i.e.*, transition state binding) and product binding.[34] We have explored the minimal requirements for effective acceleration and found that rotational freedom is surprisingly unimportant if the sites are constrained to a limited trajectory. Indeed, the accelerations and stereoselectivites achieved by the rigidly linked linear dimers would have been exciting had they been obtained before any cyclic trimer results. Flexibility emerges as a factor that is as important as equilibrium geometry, but is inevitably more elusive to characterise; excessive flexibility, as achieved by hydrogenation of the butadiyne linkers,[35] abolishes Diels–Alder acceleration altogether.[18]

One might claim that the stereochemical reversal at 30 °C is a major success for the design approach to supramolecular chemistry, but it is salutory to remember that at 60 °C the results are equivocal while at 80 °C one sees little acceleration[18,32] and would expect no stereochemical reversal. As we have pointed out previously in relation to the concentration dependence of templated synthesis, one is often delicately poised between spectacular success and dismal failure.[13] Certainly the more difficult tasks of changing regiochemistry and engineering catalytic turnover remain a challenge.

To investigate this reaction more quantitatively is a challenging objective that is severely constrained by experimental and theoretical considerations. To add to the purely practical difficulties of obtaining reliable data for this particular system is the more profound problem of demonstrating that one non-trivial kinetic model is uniquely better or worse than any other: the kinetics of host-accelerated reactions become increasingly complex when the formation rates of two different products with differing thermodynamic stabilities are accelerated by different amounts. In our system, even demonstrating whether the substrates bind selectively or randomly inside and outside is not trivial.[36] This is arguably a result of poor design in our case, but as Schneider *et al.* have noted,[37] the formal analysis of artificial catalytic host–guest systems is often more complicated than that of biological systems. Simplifications can be made in the analysis of an enzymatic system because these catalysts have become highly efficient under the pressures of natural evolution over many millions of years. As a consequence, non-catalysed and other side reactions are negligible, catalyst saturation can be achieved, and well-defined binary and ternary complexes can be assumed. Current synthetic biomimetic systems have evolved over only a short period, usually under conscious control rather than under evolutionary pressure, and are therefore often not amenable to such simplifications.

There is now a movement towards developing evolutionary and selection approaches[38] using catalytic antibodies,[1,6] imprinted polymers[39] and small molecular systems.[40,41] It remains to be seen whether these will provide a shorter route to effective catalysts.

Experimental

^{1}H NMR spectra were recorded on Bruker WM-250 or DRX-500 spectrometers in deuteriochloroform operating at 250 or 500 MHz, respectively, while ^{13}C NMR spectra were obtained on a Bruker WM-250 spectrometer operating at 62.5 MHz. Chemical shifts are quoted relative to residual solvent (7.25 ppm for ^{1}H and 77.0 ppm for ^{13}C of $CDCl_3$). Unless otherwise stated, the acquisition temperature of NMR spectra was 25($\pm$3) °C. Porphyrin ^{1}H and ^{13}C assignments were made by comparison with previously assigned, similarly substituted porphyrin species. Routine UV/VIS spectra were obtained on a Uvikon 810 spectrometer or a Hewlett Packard 8452A diode array spectrophotometer in 10 mm oven-dried cuvettes. Fast atom bombardment mass spectra (FAB MS) were recorded on a Kratos MS-50 mass spectrometer (Cambridge) or on a VG Autospec mass spectrometer (EPSRC service at Swansea).

All solvents were distilled prior to use and when used dry, were obtained fresh from solvent stills: triethylamine, toluene and dichloromethane were distilled from CaH_2 under an atmosphere of argon while tetrahydrofuran and diethyl ether were distilled from $LiAlH_4$–CaH_2, also under argon. Flash chromatography was carried out using dry-packed 60 mesh silica gel and TLC was carried out on Kieselgel 60 PF_{254} (Merck) 0.2 mm plates.

Free base porphyrins were converted into zinc complexes in near quantitative yield by treatment with zinc acetate dihydrate in refluxing chloroform (10 min) until no further change could be detected by UV inspection. Excess of zinc acetate was removed by washing twice with water before drying ($MgSO_4$) and removal of the solvent by evaporation. The final purification step in the preparation of porphyrins was crystallisation by layered addition of methanol to a chloroform solution of the compound, (or the layered addition of hexane to a dichloromethane solution), followed by drying *in vacuo*.

Dienophile 4

3,6-Epoxy-1,2,3,6-tetrahydro-*N*-(4-pyridylmethyl)phthalamic acid. 4-Aminomethylpyridine (2 ml, 20 mmol) in anhydrous THF (30 ml) was added dropwise to a solution of 3,6-epoxy-1,2,3,6-tetrahydrophthalic anhydride (2.66 g, 15 mmol) in anhydrous THF (200 ml). The solution was stirred under a drying tube at 25 °C for 12 h. The resulting precipitate was washed with tetrahydrofuran and dried *in vacuo* to afford white crystals of the product. Yield 4.22 g (78%). ^{1}H NMR (250 MHz, $CDCl_3$) δ: 2.63 (1H, d, J = 8, α to C=O), 2.65 (1H, d, J = 8, α to C=O), 4.25 (1H, dd, J = 3, 15, benzylic CH_2), 4.31 (1H, dd, J = 3, 15, benzylic CH_2), 4.96 (1H, br m, bridgehead), 5.11 (1H, br m, bridgehead), 6.46 (2H, br m, alkene protons), 7.28 (2H, d, J = 6, pyridyl), 8.22 (1H, t, J = 3, NH), 8.47 (2H, d, J = 6 Hz, pyridyl).

3,6-Epoxy-1,2,3,6-tetrahydro-*N*-(4-pyridylmethyl)phthalimide. 1-Hydroxybenzotriazole hydrate (HOBT, 2.38 g, 16.9 mmol) and *N*,*N*′-dicyclohexylcarbodiimide (DCC, 4.07 g, 18.9 mmol) were added to a solution of 3,6-epoxy-1,2,3,6-tetrahydro-*N*-(4-pyridomethyl)phthalamic acid (4.22 g, 0.015 mmol) in dry dichloromethane (300 ml) at 0 °C. The resulting mixture was stirred at this temperature under a drying tube for 2 h and then for 12 h at room temperature. Insoluble by-products were removed by filtration and the solvent subsequently removed by evaporation to give a pale brown oil. Purification by column chromatography on silica, eluting with neat chloroform, yielded the product as a white solid (2.43 g, 62%). ^{1}H NMR (250 MHz, $CDCl_3$) δ: 2.90 (2H, br m, α to C=O), 4.62 (2H, s, benzylic CH_2), 5.29 (2H, br m, bridge head), 6.51 (2H, br m, alkene protons), 7.16 (2H, d, J = 6, pyridyl), 8.52 (2H, d, J = 6 Hz, pyridyl).

4-(Maleimidomethyl)pyridine, 4. 3,6-Epoxy-1,2,3,6-tetrahydro-*N*-(4-pyridylmethyl)phthalimide (90 mg, 0.35 mmol) was heated to 160 °C at a pressure of 15 mm Hg and the product collected on a cold finger (cooled with ice water) held 2 cm above the reactant. Yield 40 mg (61%). ^{1}H NMR (250 MHz, $CDCl_3$) δ: 4.66 (2H, s, benzylic CH_2), 6.76 (2H, s, alkene protons), 7.19 (2H, d, J = 6, pyridyl), 8.55 (2H, d, J = 6 Hz, pyridyl).

Diene 3

4-Trimethylstannylpyridine. The hydrogen chloride salt of 4-bromopyridine (4.00 g, 2.05 mmol) was suspended in dry diethyl ether (15 ml) and cooled to 0 °C. Sodium bicarbonate solution ($\approx$ 1 M) was added dropwise until the effervescence subsided and the aqueous solution was basic (pH paper). The two layers were separated and the aqueous phase further extracted with diethyl ether (2 × 10 ml). The organic portions were combined and left to stand ($MgSO_4$) for 3 h in the fridge before filtering and transferring to an argon-purged flask containing 4 Å molecular sieves. *n*-Butyl lithium (10.3 ml, 0.021 mol, 2 M solution in hexane) was added to an oven-dried, argon-purged flask containing dry diethyl ether (50 ml) at −78 °C. The bromopyridine solution was then transferred *via* cannula to this reaction vessel and the resulting pale brown

solution stirred at −78 °C for 15 min before being allowed to warm up to 0 °C. Trimethyltin chloride (26.4 ml of a 1 M solution in THF, 0.0264 M) was syringed into the mixture and stirring continued at this temperature for 90 min before the addition of aqueous potassium fluoride solution (20 ml, 2 M). After stirring for 20 min at room temperature, the mixture was filtered through celite to remove the white precipitate of trimethyltin fluoride. The residue was washed with ethyl acetate and the filtrate dried ($MgSO_4$) before removing the solvent by evaporation to give a brown oil. The product was purified by column chromatography on silica, eluting with a 1 : 1 mixture of 40–60 petroleum ether : ethyl acetate to give 2.80 g of a yellow oil (56%), which was used without further purification. ^{1}H NMR (250 MHz, $CDCl_3$) δ: 0.25 (9H, s, Me), 7.30 (2H, d, J = 5, Hβ), 8.42 (2H, d, J = 5 Hz, Hα).

4-(3-Furyl)pyridine 3. Tetrakis(triphenylphosphine)-palladium (0) (125 mg, 0.108 mmol), 4-trimethylstannylpyridine (0.5 g, 2.07 mmol) and 3-bromofuran (220 ml, 2.44 mmol, 1.2 equiv) were added to a suspension of dry lithium chloride (0.359 g, 8.47 mmol) in anhydrous toluene (30 ml) and the mixture refluxed under argon for 3 days. The reaction mixture was allowed to cool to room temperature and quenched with aqueous potassium fluoride solution (20 ml, 2 M). After stirring for 20 min, the mixture was filtered through celite and the residue washed with ethyl acetate. The filtrate was washed with water (50 ml) and brine (50 ml) before drying (Na_2SO_4) and removal of the solvent by evaporation. The resulting brown oil was purified by column chromatography on silica, eluting with a 2 : 1 mixture of 40–60 petroleum ether : ethyl acetate. The desired product was eluted first and evaporated to give 0.15 g of a pale brown oil (50%). 4-Phenylpyridine was eluted immediately afterwards as a by-product. ^{1}H NMR (250 MHz, $CDCl_3$) δ: 6.73 (1H, m), 7.36 (2H, d, J = 5, Hβ, pyridyl), 7.52 (1H, m), 7.87 (1H, s), 8.58 (2H, d, J = 5 Hz, Hα, pyridyl).

3·Hydrochloride. A stream of dry hydrogen chloride gas was bubbled through a stirred solution of 4-(3-furyl)pyridine (150 mg, 1.03 mmol) in diethyl ether (25 ml). After several minutes a white precipitate of 4-(3-furyl)pyridine hydrochloride formed. The crystals were filtered off, washed with 25 ml of diethyl ether and dried *in vacuo* (165 mg, 88%).

Oligomers

$Zn_2$8. Tetrakis(triphenylphosphine)palladium (0) (7.6 mg, 0.0066 mmol) and copper(I) iodide (3 mg, 0.016 mmol) were added to a solution of mono-TMS porphyrin **Zn10** (65 mg, 0.062 mmol) and TMS-iodoporphyrin **Zn9** (72 mg, 0.062 mmol) in anhydrous THF (12 ml) and triethylamine (12 ml). The mixture was degassed (3 freeze-thaw cycles) and refluxed at 85 °C under argon for 5 h after which TLC analysis (hexane–chloroform–ethyl acetate, 2 : 1 : 1) showed only a trace of starting material left. The mixture was poured into water (50 ml) and extracted with dichloromethane (50 ml). The organic phase was further washed with water (50 ml) before drying ($MgSO_4$) and evaporating to give a red solid, which was purified by column chromatography on silica. Elution with hexane–chloroform–ethyl acetate (2 : 1 : 1 v/v) removed any remaining traces of monomer, and the product was then eluted with neat chloroform. Recrystallisation from dichloromethane–hexane yielded 88 mg of a red solid (68%). ^{1}H NMR (250 MHz, $CDCl_3$) δ: 0.25 (18H, s, TMS), 2.49, 2.54 (24H, 2 × s, Me), 3.14 (16H, t, J = 7.6, $CH_2CH_2CO_2Me$), 3.66 and 3.67 (24H, 2 × s, MeO), 4.32 (16H, t, J = 7.6 Hz, $CH_2CH_2CO_2Me$), 7.65–8.31 (16H, m, aryl-H), 10.19 (4H, s, *meso*-H); ^{13}C NMR (62.5 MHz, APT, $CDCl_3$) δ: 0.02 (Me, TMS), 15.65 (Me), 21.91, 36.94 (CH_2), 51.69 (MeO), 89.99, 94.67 (C≡*C*—aryl), 97.45 (*meso*-H), 105.02 (C≡*C*—TMS), 127.61, 127.83, 131.52, 131.66, 131.93, 133.09, 136.14, 136.36 (aryl-H), 118.75, 122.71, 138.37, 139.03, 141.53, 143.33, 143.66, 143.71, 146.03, 147.61 (quaternary pyrrole and aryl carbons), 173.5 (ester C=O); UV/VIS (CH_2Cl_2) λ_{max}/nm: 334.1, 409.2, 539.7, 574.6; MALDI-TOF MS ($C_{116}H_{118}N_8O_{16}Si_2Zn_2$) calculated: 2067.1832, found: 2069; FAB MS: 2065 $[M-2]^+$, 2067 $[M]^+$, 2089 $[M+Na]^+$.

$Zn_2$11. Palladium on charcoal (250 mg, 10%) was added to a solution of **$Zn_2$8** (70 mg, 0.034 mmol) in anhydrous THF (150 ml). The mixture was purged with hydrogen and stirred for 12 h under a slight positive pressure of hydrogen. The catalyst was removed by filtration through celite and the solvent evaporated under reduced pressure to give a red solid that was recrystallised from chloroform–methanol (40 mg, 57%). ^{1}H NMR (250 MHz, $CDCl_3$) δ: 0.08 (18H, s, TMS), 1.08 (4H, m, CH_2-TMS), 2.30, 2.31, 2.37, 2.47, 2.56 (24H, 5 × s, Me), 2.78–2.85 (8H, m, CH_2-aryl), 3.12–3.36 (16H, m, $CH_2CH_2CO_2Me$), 3.44, 3.61, 3.65, 3.66, 3.67 (24H, 5 × s, MeO), 3.97–4.30 (16H, m, $CH_2CH_2CO_2Me$), 7.54–7.96 (16H, m, aryl-H), 10.08, 10.10, 10.20 (4H, 3 × s, *meso*-H); ^{13}C NMR (62.5 MHz, APT, $CDCl_3$) δ: 1.01 (Me, TMS), 15.25, 15.15 (Me), 19.33, 21.70, 21.97, 30.31, 36.63, 36.70, 36.99 (CH_2), 51.42, 51.64 (MeO), 97.04 (*meso*-H), 127.60, 127.74, 128.74, 130.31, 130.41, 131.04, 132.83, 133.52 (aryl-H), 112.63, 120.21, 139.17, 139.29, 140.81, 141.00, 141.05, 141.20, 143.12, 143.35, 144.81, 145.85, 145.95, 147.70 (quaternary pyrrole and aryl carbons), 173.32, 173.56 (ester C=O); FAB MS ($C_{116}H_{130}N_8O_{16}Si_2Zn_2$) calculated: 2079.28, found: 2079; $[M]^+$, 2080 $[M+H]^+$; UV/VIS (CH_2Cl_2) λ_{max}/nm: 332.0, 409.2, 502.9, 574.4.

$Zn_3$12 (TMS-protected linear trimer). A solution of diiodo porphyrin monomer **Zn14** (59 mg, 0.050 mmol) and mono-TMS porphyrin **Zn10** (110 mg, 0.105 mmol, 2.1 equiv) in THF–triethylamine (35 ml : 7 ml) was degassed (2 × freeze-thaw cycles) and heated to 35 °C under argon. Triphenylarsine (37 mg, 0.12 mmol) and tris(dibenzylideneacetone)dipalladium-(0) (14 mg, 0.015 mmol) were added and the mixture flushed through with argon for 5 min. The mixture was heated at 35 °C for 90 min before removal of the solvent by rotary evaporation to give a red solid. This was chromatographed on silica, eluting initially with hexane–ethyl acetate–chloroform (2 : 1 : 1 v/v) to remove any monomers, followed by neat chloroform to remove the product, which developed as a red band. Recrystallisation from dichloromethane–hexane yielded pure product (103 mg, 68%) identical to authentic material.[21]

^{1}H NMR assay for kinetic analysis of the Diels–Alder reaction

[$^2H_2$]-1,1,2,2-Tetrachloroethane was deacidified by standing over potassium carbonate for 24 h. The host and substrates were weighed out using a six-figure balance and each made up to a concentration of 9×10^{-4} M. The hydrochloride salt of the diene was deacidified by stirring in tetrachloroethane over potassium carbonate for 2 h before filtering through a cotton wool plug. The host and the reactant solutions were then combined and transferred to a small Schlenk tube in a Grant LTD6 constant-temperature water bath. Solutions that were to be left for a long period of time were flushed with argon prior to immersion.

Samples (0.4 ml) of the reaction mixture were removed at regular intervals using a 1 ml disposable syringe with a 6″ 18SWG needle and transferred to a small vial. [$^2H_1$]Trifluoroacetic acid–[$^2H_4$]methanol (1 : 1, 0.2 ml) was added, resulting in a colour change from red to dark green. After stirring at room temperature for 10 min, the solution

was neutralised by the addition of potassium carbonate (3 microspatula tips). On stirring for a further 15 min the solution turned red once more and the potassium carbonate was removed by filtration through a cotton wool plug. [$^2H_5$]Pyridine (100%, 2 drops) was added to ensure complete neutralisation and the samples were then analysed by 500 MHz ^{1}H NMR spectroscopy.

Measurement of binding constants

All UV cuvettes, volumetric flasks and syringes were dried *in vacuo* prior to use. Dichloromethane was freshly distilled (ex. CaH_2) and tetrachloroethane was deacidified by passing through a short column of basic alumina (Brockmann grade III) and storing over potassium carbonate. All UV titrations were carried out using a Hewlett-Packard 8452A diode array spectrometer fitted with a heating jacket (estimated error in temperature $\pm 0.1\,^{\circ}C$). Other experimental details and data analysis were as described previously.[26]

Acknowledgements

We thank P. Ribereau and G. Queguiner (Rouen) for helpful advice concerning the synthesis of furylpyridine **3**, the EPSRC mass spectrometry service for FAB spectra, and European Union HCM and TMR Programs, NSERC Canada and EPSRC for financial support.

References

1 See for example T. Li, R. A. Lerner and K. Janda, *Acc. Chem. Res.*, 1997, **30**, 115; P. Wentworth, Jr., A. Datta, S. Smith, A. Marshall, L. J. Partridge and G. M. Blackburn, *J. Am. Chem. Soc.*, 1997, **119**, 2315.
2 R. Breslow and C. Schmuck, *J. Am. Chem. Soc.*, 1996, **118**, 6601; R. Breslow, J. Desper and Y. Huang, *Tetrahedron Lett.*, 1996, **37**, 2541.
3 In this shorthand notation, each number signifies the number of acetylene units in the porphyrin-porphyrin link. Thus **Zn$_3$1** is the 1,1,2-trimer and **Zn$_3$2** is the 2,2,2-trimer.
4 W. L. Mock, T. A. Irra, J. P. Wepsiec and M. Adhya, *J. Org. Chem.*, 1989, **54**, 5302.
5 W.-S. Chung, N.-J. Wang, Y.-D. Liu, Y.-J. Leu and M. Y. Chiang, *J. Chem. Soc., Perkin Trans. 2*, 1995, 307.
6 V. E. Gouverneur, K. N. Houk, B. Depascualteresa, B. Beno, K. D. Janda and R. A. Lerner, *Science*, 1993, **262**, 204; M. Resmini, A. A. P. Meekel and U. K. Pandit, *Pure Appl. Chem.*, 1996, **68**, 2025.
7 F. Fringuelli and A. Taticchi, *Dienes in the Diels–Alder Reaction*, Wiley, Chichester, 1990.
8 R. Breslow and D. C. Rideout, *J. Am. Chem. Soc.*, 1980, **102**, 7816; N. K. Sangwan and H.-J. Schneider, *Angew. Chem., Int. Ed. Engl.*, 1987, **26**, 896; V. K. Singh, B. N. S. Raju and P. T. Deota, *Synth. Commun.*, 1988, **18**, 567; P. A. Grieco, P. Garner and Z. He, *Tetrahedron Lett.*, 1983, **24**, 1897; D. A. Jaeger and J. Wang, *Tetrahedron Lett.*, 1992, **33**, 6415.
9 A. D. Hamilton and S. C. Hirst, *J. Am. Chem. Soc.*, 1991, **113**, 382; T. R. Kelly, V. S. Ekkundi and P. Meghani, *Tetrahedron Lett.*, 1990, **31**, 3381; J. Rebek, Jr. and J. Kang, *Nature* (*London*), 1997, **385**, 50.
10 For a self-replicating Diels–Alder reaction see B. Wang and I. O. Sutherland, *Chem. Commun.*, 1997, 1495.
11 K. Endo, K. Takashi, T. Sawaki, O. Hayashida, H. Masuda and Y. Aoyama, *J. Am. Chem. Soc.*, 1997, **119**, 4117.
12 D. Hilvert, K. W. Hill, K. D. Nared and M.-T. M. Auditor, *J. Am. Chem. Soc.*, 1989, **111**, 9261.
13 J. K. M. Sanders, *Comprehensive Supramolecular Chemistry*, eds. J. L. Atwood, J. E. D. Davies, D. D. Macnicol and F. Vögtle, Elsevier, Oxford, 1996, vol. 9, pp. 131–164.
14 H. L. Anderson and J. K. M. Sanders, *J. Chem. Soc., Perkin Trans. 1*, 1995, 2223.
15 C. J. Walter, H. L. Anderson and J. K. M. Sanders, *J. Chem. Soc., Chem. Commun.*, 1993, 458.
16 R. P. Bonar-Law, L. G. Mackay, C. J. Walter, V. Marvaud and J. K. M. Sanders, *Pure Appl. Chem.*, 1994, **66**, 803.
17 C. J. Walter and J. K. M. Sanders, *Angew. Chem., Int. Ed. Engl.*, 1995, **34**, 217.
18 C. J. Walter, Ph.D. Thesis, University of Cambridge, 1994.
19 Early Diels–Alder experiments[15–18] were carried out with the ethyl sidechain version of **Zn$_3$2**; recent results are from the more soluble propionate ester sidechain version. The latter is slightly more effective in accelerating the Diels–Alder reaction than the original trimer by virtue of larger binding constants and a larger effective molarity for the reaction within the cavity but the stereoselectivity is unchanged.[18]
20 A. Vidal-Ferran, C. M. Müller and J. K. M. Sanders, *J. Chem. Soc., Chem. Commun.*, 1994, 2657; structure correction: *ibid.*, 1996, 1849.
21 A. Vidal-Ferran, N. Bampos and J. K. M. Sanders, *Inorg. Chem.*, 1997, **36**, 6117.
22 P. Ribereau and G. Queguiner, *Can. J. Chem.*, 1983, **61**, 334.
23 S. Anderson, H. L. Anderson and J. K. M. Sanders, *J. Chem. Soc., Perkin Trans. 1*, 1995, 2247.
24 **Zn$_2$7** was also hydrogenated to give the even more flexible —$CH_2CH_2CH_2CH_2$— linked linear dimer but this showed no significant Diels–Alder acceleration and was not explored further.
25 J. C. Hawley, Z. Clyde-Watson and J. K. M. Sanders, unpublished results.
26 H. L. Anderson, S. Anderson and J. K. M. Sanders, *J. Chem. Soc., Perkin Trans. 1*, 1995, 2231.
27 Diene and dienophile binding constants for **Zn$_2$11** were approximately half the size as for other hosts, presumably because the flexible dimer can partly self-associate through intramolecular π–π interactions, thereby reducing the affinity for external ligands: C. A. Hunter, M. N. Meah and J. K. M. Sanders, *J. Am. Chem. Soc.*, 1990, **112**, 5773.
28 A. Vidal-Ferran, Z. Clyde-Watson, N. Bampos and J. K. M. Sanders, *J. Org. Chem.*, 1997, **62**, 240.
29 Z. Clyde-Watson, Ph.D. Thesis, University of Cambridge, 1997.
30 S. J. Webb, Z. Clyde-Watson, N. Bampos and J. K. M. Sanders, in preparation.
31 R. S. Wylie and J. K. M. Sanders, *Tetrahedron*, 1995, **51**, 513.
32 D. W. J. McCallien, Ph.D. Thesis, University of Cambridge, 1995.
33 Two substrates can be arranged productively in two ways on two binding sites, but in six ways on three binding sites.
34 More extensive studies on a range of substituted 2,2,2-trimers have quantified this linear free energy relationship.[18,32]
35 N. Bampos, V. Marvaud and J. K. M. Sanders, *Chem. Eur. J.*, 1998, **4**, 335.
36 R. S. Wylie, E. G. Levy and J. K. M. Sanders, *Chem. Commun.*, 1997, 1611.
37 H.-J. Schneider, R. Kramer and J. Rammo, *J. Am. Chem. Soc.*, 1993, **115**, 8980.
38 P. A. Brady and J. K. M. Sanders, *Chem. Soc. Rev.*, 1997, **26**, 327.
39 G. Wulff, T. Gross and R. Schonfeld, *Angew. Chem., Int. Ed. Engl.*, 1997, **36**, 1962.
40 S. J. Rowan and J. K. M. Sanders, *Chem. Commun.*, 1997, 1407; P. A. Brady and J. K. M. Sanders, *J. Chem. Soc., Perkin Trans. 1*, 1997, 3237.
41 P. G. Swann, R. A. Casanova, A. Desai, M. M. Frauenhoff, M. Urbancic, U. Slomczynka, A. J. Hopfinger, G. C. Le Breton and D. L. Venton, *Biopolymers*, 1996, **40**, 617.

Received in Montpellier, France, 2nd December 1997;
Paper 7/09199K